Lipid Profiling of the Arabidopsis Hypersensitive Response Reveals Specific Lipid Peroxidation and Fragmentation Processes: Biogenesis of Pimelic and Azelaic Acid[1][C][W]

Maria Zoeller, Nadja Stingl, Markus Krischke, Agnes Fekete, Frank Waller, Susanne Berger, and Martin J. Mueller*

Julius-von-Sachs-Institute of Biosciences, Biocenter, Pharmaceutical Biology, University of Wuerzburg, D–97082 Wuerzburg, Germany

Lipid peroxidation (LPO) is induced by a variety of abiotic and biotic stresses. Although LPO is involved in diverse signaling processes, little is known about the oxidation mechanisms and major lipid targets. A systematic lipidomics analysis of LPO in the interaction of Arabidopsis (*Arabidopsis thaliana*) with *Pseudomonas syringae* revealed that LPO is predominantly confined to plastid lipids comprising galactolipid and triacylglyceride species and precedes programmed cell death. Singlet oxygen was identified as the major cause of lipid oxidation under basal conditions, while a 13-lipoxygenase (LOX2) and free radical-catalyzed lipid oxidation substantially contribute to the increase upon pathogen infection. Analysis of *lox2* mutants revealed that LOX2 is essential for enzymatic membrane peroxidation but not for the pathogen-induced free jasmonate production. Despite massive oxidative modification of plastid lipids, levels of nonoxidized lipids dramatically increased after infection. Pathogen infection also induced an accumulation of fragmented lipids. Analysis of mutants defective in 9-lipoxygenases and LOX2 showed that galactolipid fragmentation is independent of LOXs. We provide strong in vivo evidence for a free radical-catalyzed galactolipid fragmentation mechanism responsible for the formation of the essential biotin precursor pimelic acid as well as of azelaic acid, which was previously postulated to prime the immune response of Arabidopsis. Our results suggest that azelaic acid is a general marker for LPO rather than a general immune signal. The proposed fragmentation mechanism rationalizes the pathogen-induced radical amplification and formation of electrophile signals such as phytoprostanes, malondialdehyde, and hexenal in plastids.

Lipid peroxidation (LPO), triggered by lipoxygenases (LOX) and reactive oxygen species (ROS), is a hallmark of plant pathogen responses, both in signal transduction processes and during the execution of programmed cell death. Typically, LOX oxidize free fatty acids in the cytosol or chloroplasts, thereby initiating several oxylipin pathways including the jasmonate and hydroperoxide lyase pathway (Mosblech et al., 2009). Among the ROS typically produced in plant stress responses, only singlet oxygen ($^1O_2$) and free radicals are sufficiently reactive to oxidize polyunsaturated fatty acids directly (Mueller et al., 2006). These short-lived ROS produced in different cellular compartments, including plasma membrane, plastids, mitochondria, peroxisomes, endoplasmic reticulum, and cytosol, are thought to oxidize predominantly glycerolipids close to the site of ROS production. In a recent study, $^1O_2$ was shown to be a major ROS species involved in photooxidative lipid oxidation and damage in Arabidopsis (*Arabidopsis thaliana*) leaves (Triantaphylidès et al., 2008). However, the major sites and molecular targets of lipid oxidation as well as the relative contributions of different ROS species and LOXs to LPO and fragmentation have not been clarified.

LOXs and ROS have also been implicated in the formation of fragmented fatty acids in plants and animals. Pathways for enzymatic and nonenzymatic fatty acid peroxide cleavage yielding two aldehyde fragments have been described in plants and animals (Fig. 1). The enzymatic fragmentation pathway (Fig. 1A), which has been described in plants only, involves LOX and hydroperoxide lyases (HPL) acting on free fatty acids (Matsui et al., 2006). One aldehyde fragment harbors the fatty acid carboxylate group (oxo-fatty acid), while the other aldehyde fragment containing the fatty acid methyl end is released as a volatile compound. Finally, oxo-fatty acids can be oxidized by aldehyde dehydrogenase (Kirch et al., 2005; Mukhtarova et al., 2011), yielding dicarboxylic acids. Arabidopsis ecotype

[1] This work was supported by the Deutsche Forschungsgemeinschaft (grant nos. GK1342 and SFB567).

* Corresponding author; e-mail martin.mueller@biozentrum.uni-wuerzburg.de.

The author responsible for distribution of materials integral to the findings presented in this article in accordance with the policy described in the Instructions for Authors (www.plantphysiol.org) is: Martin J. Mueller (martin.mueller@biozentrum.uni-wuerzburg.de).

[C] Some figures in this article are displayed in color online but in black and white in the print edition.

[W] The online version of this article contains Web-only data.

www.plantphysiol.org/cgi/doi/10.1104/pp.112.202846

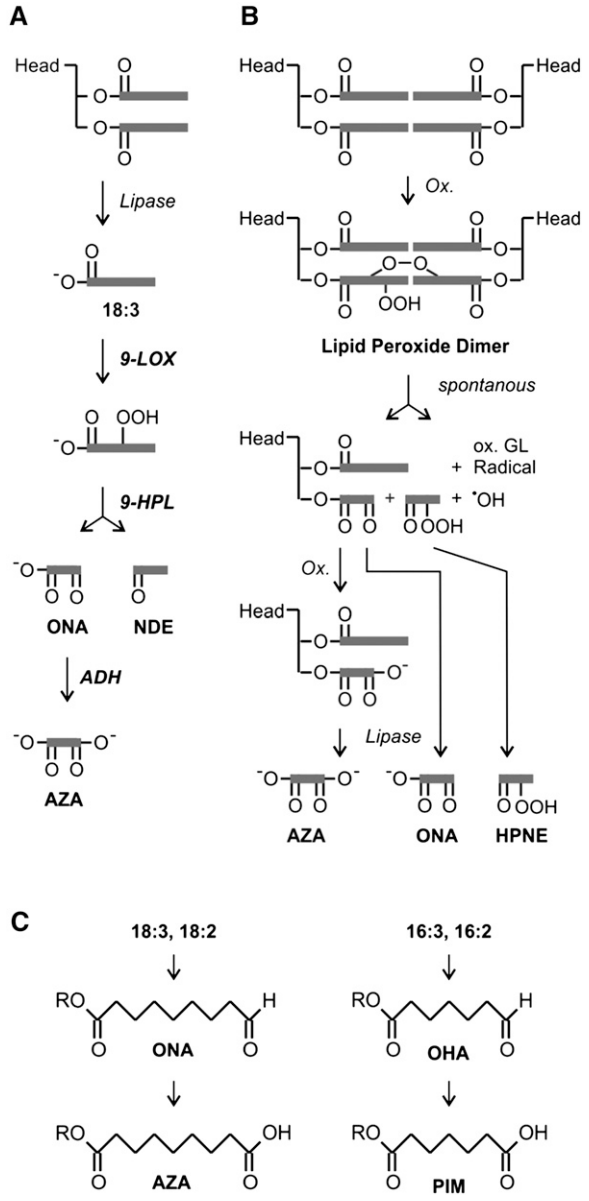

Figure 1. Fatty acid fragmentation pathways. A, Enzymatic oxidative fragmentation of 18:3 via 9-LOX, 9-HPL, and aldehyde dehydrogenase (ADH), yielding ONA, nonadienal (NDE), and AZA (Matsui, 2006). Gray bars represent the carbohydrogen backbone of fatty acids. B, Radical-catalyzed oxidative fragmentation of esterified 18:2 in glycerolipids via the dimer pathway, yielding oxidized glycerolipids (GL), ONA, AZA, and hydroperoxynonenal (HPNE) in animals (Schneider et al., 2008). C, Structures of predicted carboxylic acidic fragments generated through the dimer pathway from different plant polyunsaturated fatty acids: ONA, AZA, OHA, and PIM.

Columbia (Col-0), however, lacks 9-HPL genes, and the 13-HPL gene has been shown to be mutated and nonfunctional (Matsui et al., 2006; Chehab et al., 2008). Since Arabidopsis Col-0 produces fatty acid fragments such as azelaic acid, another yet unknown fragmentation pathway must be operative (Jung et al., 2009).

A nonenzymatic fatty acid fragmentation pathway has been described in vitro and in animals in vivo (Fig. 1B). In animals, fatty acid peroxide fragmentation is catalyzed by free radicals and has been shown to take place in phospholipids and cardiolipins in vivo under oxidative stress conditions (Hazen and Chisolm, 2002; Hazen, 2008). The nonenzymatic mechanism produces a variety of aldehyde fragments from different fatty acid peroxides, including those aldehydes produced by plant HPL enzymes. After radical-induced fragmentation of mammalian glycerolipids, however, the oxo-acid fragment remains esterified in the membrane while the other fragment is released from the membrane. Oxidatively fragmented phospholipids were shown to serve as endogenous pattern-recognition ligands that activate the innate immune system of animals in trace amounts (Hazen, 2008). However, such fragmented glycerolipids have not yet been described in plants.

The nonenzymatic fragmentation mechanism has been investigated in detail (Schneider et al., 2008) and shown to proceed through lipid peroxide dimers that spontaneously undergo fragmentation (Fig. 1B). The main fragmented fatty acids found esterified in mammalian glycerolipids are the C_9-oxo-acid fragments 9-oxononanoic acid (ONA) and azelaic acid (AZA) and the C_7 fragments 7-oxoheptanoic acid (OHA) and pimelic acid (PIM). We hypothesized that C_9 and C_7 fragments could be generated in planta by free radical-catalyzed cleavage of esterified polyunsaturated C18 and C16 fatty acids, respectively (Fig. 1C).

Interest in the fragmentation pathway stems from the fact that several short-chain aldehyde fragments (i.e. malondialdehyde, hydroxynonenal, and hexenal) are potent electrophiles that function as stress signals (Farmer and Davoine, 2007) in plants. Important functions for dicarboxylic acids have also been reported. For instance, PIM is an essential precursor of biotin. PIM biosynthesis has only recently been clarified in bacteria (Lin et al., 2010), and there is yet no evidence that an enzymatic pathway is operative in Arabidopsis. Another dicarboxylic acid, AZA, has recently been identified as a pathogen-induced metabolite in Arabidopsis vascular sap that has been reported to confer local and systemic resistance against the pathogen *Pseudomonas syringae* (*Pst*; Jung et al., 2009; Chaturvedi et al., 2012). AZA was also proposed to prime plants to accumulate salicylic acid, a defense signal involved in systemic acquired resistance (SAR) upon infection. Since AZA can be transported in the vascular sap, it was suggested to be a long-distance systemic signal in plants (Shah, 2009). Mutation of the *AZELAIC ACID INDUCED1* (*AZI1*) gene, which was induced by AZA, results in the loss of systemic immunity triggered by pathogens or AZA (Jung et al., 2009). However, direct genetic proof for a function of AZA in defense signaling is still missing. In the case of an enzymatic AZA biosynthesis, analysis of mutants deficient in AZA biosynthesis would be one approach to test the function of AZA.

In this study, a systematic analysis of pathogenesis-associated LPO in plants identified plastidic monogalactosyldiacylglycerols and digalactosyldiacylglycerols

(MGDG and DGDG) as well as triacylglycerols (TG) as major oxidized glycerolipids in Arabidopsis leaves. Detailed analysis of lipid oxidation products in the wild type and mutants related to lipid metabolism allowed us to clarify different oxidation mechanisms involved in LPO and fragmentation in vivo, thereby identifying the biogenesis of oxidized lipids in the plant response to abiotic and biotic stress. We also present a model explaining the formation of reactive electrophile species previously shown to be involved in important plant signaling processes.

RESULTS

Oxidized Fatty Acids and Fragmented Fatty Acids Increase in Arabidopsis Leaves after Infection with Avirulent *Pst* Bacteria

In order to investigate the kinetics of lipid oxidation, leaves of 6-week-old Arabidopsis plants were infiltrated with an avirulent or a virulent strain of *Pst* DC3000 (10^8 colony-forming units [cfu] mL^{-1}), and the accumulation of enzymatically and nonenzymatically formed oxidized lipids was monitored at different time points. As shown in Figure 2, levels of several oxidized fatty acids including AZA and PIM were elevated 5 to 10 h after infection with the avirulent strain and reached highest levels at 24 h, when the leaves showed severe visible damage. Levels of the established marker (Mueller et al., 2006; Grun et al., 2007) of nonenzymatic 18:3 oxidation, 16-hydroxyoctadecatrienoic acid (16-HO-18:3), increased with AZA and PIM as early as 5 to 10 h and reached 5- to 10-fold elevated levels after 24 h. In parallel, levels of jasmonic acid (JA) synthesized via the 13- LOX pathway were also and even more dramatically upregulated (over 75-fold) within 5 to 10 h post infection. In contrast, infection with the virulent *Pst* strain (10^8 cfu mL^{-1}) induced only a low accumulation of all tested oxidized fatty acids, and visible damages were barely detectable after 24 h. Infection experiments with lower bacterial densities of the avirulent *Pst* strain (10^6 and 10^7 cfu mL^{-1}) revealed that levels of oxidized lipids and visible leaf damage were lower, likely due to the delayed cell death response (Supplemental Fig. S1A). All lipids analyzed were from plant origin and not detectable in both *Pst* strains. Both early nonenzymatic and enzymatic oxylipin biosynthesis preceded visible leaf damage and increased until cell death occurred (Fig. 2; Supplemental Fig. S1B). However, we could not detect ONA or OHA, the putative precursors of AZA and PIM (Fig. 1), respectively.

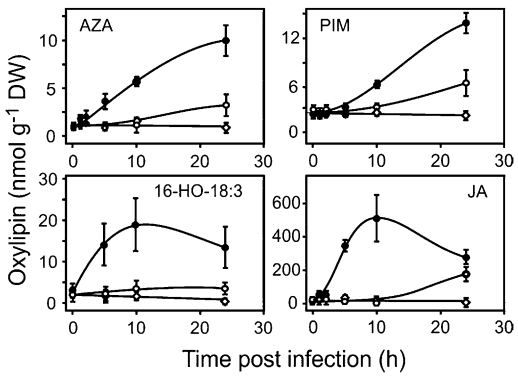

Figure 2. Pathogen-induced accumulation of oxidized free fatty acids in Arabidopsis leaves. Levels of AZA and PIM together with levels of markers of nonenzymatic lipid oxidation (16-HO-18:3) and enzymatic lipid oxidation (JA) are shown after infection with avirulent (black circles) and virulent (white circles) *Pst* (10^8 cfu mL^{-1}) or mock infiltration (diamonds). Values shown are means ± SD (n = 3). DW, Dry weight.

9-LOX, Trienoic Fatty Acids, and AZI1 Are Not Essential for AZA and PIM Biogenesis

It has been proposed that the 9-LOX pathway (Fig. 1A) is essential for the formation of AZA in planta. Arabidopsis expresses two 9-LOX proteins (LOX1 and LOX5). However, single and double transfer-DNA insertion lines (*lox1*, *lox5*, and *lox1/lox5*) of both genes in the Arabidopsis ecotype Wassilewskija, which are completely deficient in the respective 9-LOX activities (Vellosillo et al., 2007; López et al., 2011), accumulated wild-type levels of AZA and PIM after infection with the avirulent *Pst* (Fig. 3A). Hence, enzymatic formation of AZA and PIM through the 9-LOX pathway can be ruled out. In addition, LOX2, the most abundant 13-LOX, is also not essential for lipid fragmentation (Fig. 3B).

In addition to 9-LOX, the plastidic *FATTY ACID DESATURASE7* (*FAD7*) and *AZI1* have been suggested to be involved in the local production or transport of AZA and/or the SAR signal, respectively (Chaturvedi et al., 2008; Jung et al., 2009). Therefore, we tested mutants deficient in these genes for their capacity to accumulate AZA and PIM in infected leaves. As shown in Figure 3B, local production of AZA and PIM was not compromised in the fatty acid desaturase triple mutant *fad3-2 fad7-2 fad8* and *azi1*. In the *fad3-2 fad7-2 fad8* triple mutant, trienoic fatty acids are quantitatively replaced by dienoic fatty acids (McConn and Browse, 1996) that may, however, also serve as precursors for fragmented fatty acids.

Previously, it has been suggested that AZA is transported to noninfected systemic leaves after *Pst* infection (Jung et al., 2009). However, AZA and PIM levels in systemic leaves 24 h post infection were not elevated and were comparable to levels in leaves of noninfected wild-type and mutant plants (Fig. 3; Supplemental Fig. S1B). Moreover, we observed that the *AZI1* gene, which was reported to be induced by AZA and required for the SAR response (Jung et al., 2009), was not induced by AZA. Although a weak and transient induction of *AZI1* after spraying of AZA (in MES buffer) could be measured as reported by Jung et al. (2009), this induction was also seen after spraying of buffer alone (Supplemental Fig. S2A). More importantly, however, AZA pretreatment of Arabidopsis leaves (as described by Jung et al. [2009]) did

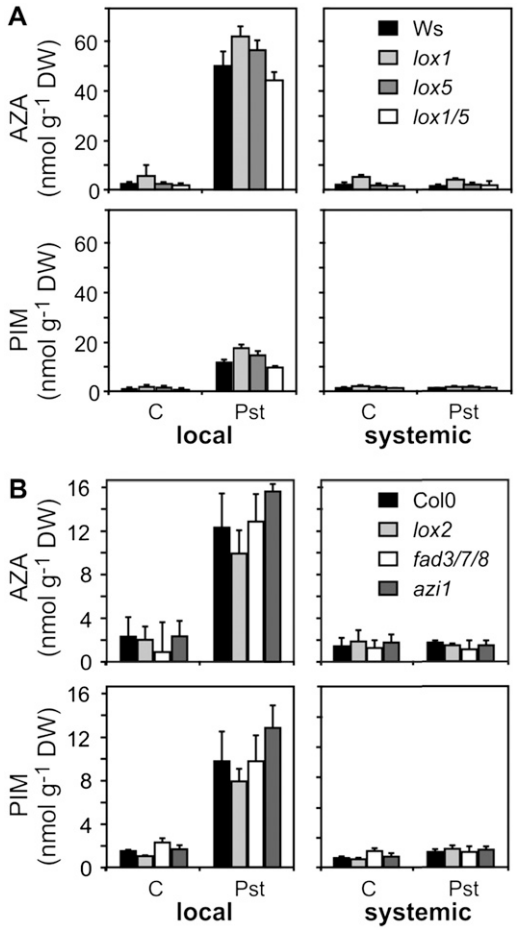

Figure 3. Pathogen-induced increase of AZA and PIM in Arabidopsis. Levels of AZA and PIM were determined 24 h after infection of Arabidopsis leaves with avirulent *Pst* (10^8 cfu mL^{-1}) or mock infiltration (C). A, The single (*lox1* and *lox5*) and double (*lox1/5*) 9-LOX insertion lines were compared with the corresponding wild type (accession Wassilewskija [Ws]). B, The mutant lines *lox2*, *fad3 fad7 fad8* (*fad3/7/8*), and *azi1* were compared with the respective wild-type Col-0. Values shown are means ± SD ($n = 3$). DW, Dry weight.

not inhibit the growth of spray-inoculated virulent *Pst* under our experimental conditions (Supplemental Fig. S2B).

AZA, PIM, and Their Precursors Occur Esterified in Oxidized MGDG and DGDG in Vivo and Accumulate after *Pst* Infection

As an alternative to the enzymatic formation of AZA and PIM (Fig. 1A), free radical-catalyzed fragmentation of oxidized glycerolipids could take place, as has been observed in animals (Fig. 1B). In vitro, free radical oxidation experiments with unsaturated fatty acids revealed that 18:3 and 18:2, but not 18:1, yielded ONA and AZA (Supplemental Fig. S3). In agreement with the proposed chemical fragmentation mechanism (Schneider et al., 2008), the kinetics of the 18:3 and 18:2 oxidation products suggested that at least three oxidation events are required to produce AZA from 18:3 or 18:2: first, a fatty acid (or acyl) hydroperoxide is formed that, under radical catalysis, fragments to yield ONA. Finally, ONA is oxidized in a radical-catalyzed process to AZA (Supplemental Fig. S3). We also performed in vitro autoxidation experiments with either 9- or 13-HOO-18:3 (for hydroperoxyoctadecatrienoic acid) and observed that both peroxides nonenzymatically fragment to produce 1 to 2.5 mol % ONA and 0.3 to 0.8 mol % AZA (Supplemental Fig. S3).

The free radical-catalyzed AZA biogenesis hypothesis (Fig. 1B) predicts that 18:3 hydroperoxides, ONA and AZA, are formed by oxidation of esterified 18:3 in glycerolipids. In addition, 16:3 hydroperoxides, OHA and PIM, would be expected to be formed by oxidation of esterified 16:3 in glycerolipids. Therefore, we performed a systematic analysis of glycerolipids by ultra-performance liquid chromatography (UPLC) coupled to quadrupole-time of flight mass spectrometry. After reduction of peroxides to the corresponding hydroxides, parent lipid molecules were determined that released fragments indicative for the presence of HO-18:3, HO-16:3, ONA, OHA, AZA, and PIM upon collision-induced fragmentation. ONA, OHA, AZA, and PIM [along with the predicted HO(O)-18:3/16:3 precursor fatty acids, where HO(O) is either hydroperoxy or hydroxy] could be identified only esterified in MGDG and DGDG (Table I). In order to determine the basal and pathogen-induced levels of these oxidized glycerolipids, a targeted analysis of the most abundant galactolipid species was performed by UPLC-tandem mass spectrometry (MS/MS) in the multiple reaction monitoring mode (for details, see "Materials and Methods"). The complex data set is shown in Table I. Under control conditions (mock infiltration), oxidized (18:3, 18:3)MGDG and DGDG contained 0.6 mol % ONA and about 0.05 mol % AZA relative to the nonoxidized precursor. Oxidized (18:3, 16:3)MGDG and DGDG contained, in addition to 18:3-derived ONA (1.6–2.5 mol %) and AZA (0.04 mol %), also 16:3-derived OHA (0.7 mol %) and PIM (0.2 mol %).

After pathogen infection, levels of both nonoxidized as well as peroxidized or fragmented galactolipids increased on average about 2-fold. Therefore, the degree of oxidation of different galactolipid species expressed in mol % relative to the nonoxidized precursor galactolipid did not change dramatically (Table I). Under control conditions, total levels of ONA, OHA, AZA, and PIM in the four major galactolipid species per g dry weight were 169, 44, 6, and 10 nmol, respectively. The presence of esterified fragmented fatty acids was also confirmed by analysis of total lipid extracts before and after alkaline hydrolysis. This analysis confirmed that ONA and OHA are only present in esterified but not in free form, while AZA and PIM are present in Arabidopsis leaves both in esterified and free form (Supplemental Fig. S4).

These findings (Table I) are in agreement with the free radical hypothesis of galactolipid fragmentation in plastids in situ (Fig. 1B). Alternatively, fatty acids are fragmented first, followed by esterification into galactolipids.

Evidence for Acyl Chain Fragmentation in Galactolipids

In order to investigate the possibility of incorporation of ONA or AZA into galactolipids, feeding experiments using [8,8-D_2]ONA and unlabeled AZA were performed. [8,8-D_2]ONA (100 μM) was applied to the medium of Arabidopsis seedlings (10 d) grown in liquid medium. After different time points, seedlings were washed and lipids were extracted and analyzed by UPLC-MS/MS. In seedling extracts, labeled ONA could not be detected at any time, indicating that ONA does not accumulate in free form (Fig. 4A). Instead, 1.5 h after [8,8-D_2]ONA application, [2,2-D_2)AZA and [2,2-D_2]PIM accumulated in the seedlings and reached levels of 130 and 55 nmol g^{-1} dry weight, respectively.

Table I. *Levels of oxidized glycerolipids and their precursors*

Levels are shown 24 h after mock infiltration (control) or *Pst* (10^8 cfu mL^{-1}) infection of Arabidopsis leaves. Lipids were analyzed by UPLC-MS/MS in the multiple reaction monitoring mode (for details, see "Materials and Methods"). Data presented as mol % indicate levels of oxidized lipids relative to the levels of the corresponding nonoxidized galactolipid species. Data (means ± SD; $n = 3$) are shown for the nonoxidized precursor lipids (boldface) and their oxidized species. ND, Not detected.

Lipid Class	Fatty Acids	Control	Avirulent *Pst*, 24 h Post Infection	Fold Increase	Basal Oxidation	*Pst* Oxidation
		nmol g^{-1} dry wt			*mol %*	
MGDG	**18:3, 18:3**	3,607 ± 340	8,832 ± 648	2.4		
	18:3, HO-18:3	58 ± 16	151 ± 43	2.6	1.6	1.7
	HO-18:3, HO-18:3	7 ± 2	56 ± 18	8.0	0.2	0.6
	18:3, ONA	21 ± 3	42 ± 12	2.0	0.6	0.5
	18:3, AZA	2 ± 0.4	7 ± 0.8	3.5	0.06	0.08
MGDG	**18:3,16:3**	5,480 ± 176	17,980 ± 296	3.3		
	HO-18:3, 16:3	502 ± 135	928 ± 261	1.8	9.2	5.2
	18:3, HO-16:3	503 ± 112	832 ± 208	1.7	9.2	4.6
	HO-18:3, HO-16:3	42 ± 16	336 ± 68	8.0	0.8	1.9
	18:3, OHA	40 ± 12	80 ± 22	2.0	0.7	0.4
	ONA, 16:3	88 ± 22	132 ± 32	1.5	1.6	0.7
	18:3, PIM	10 ± 3	15 ± 6	1,5	0.2	0.08
	AZA, 16:3	2 ± 0.8	11 ± 2	5.5	0.04	0.06
DGDG	**18:3, 18:3**	7,275 ± 552	10,052 ± 1726	1.4		
	18:3, HO-18:3	509 ± 45	814 ± 172	1.6	7.0	8.1
	HO-18:3, HO-18:3	49 ± 15	196 ± 36	4.0	0.7	1.9
	18:3, ONA	46 ± 16	58 ± 4	1.0	0.6	0.6
	18:3, AZA	2 ± 0.8	3 ± 1	1.4	0.03	0.03
DGDG	**18:3, 16:3**	559 ± 67	1,227 ± 88	2.2		
	HO-18:3, 16:3	45 ± 7	104 ± 12	2.3	8.1	8.5
	18:3, HO-16:3	58 ± 5	93 ± 20	1.6	10.4	7.6
	HO-18:3, HO-16:3	ND	ND			
	18:3, OHA	4 ± 0.8	5 ± 0.4	1.3	0.7	0.4
	ONA, 16:3	14 ± 3	11 ± 1	0.8	2.5	0.9
	18:3, ONA	ND	ND			
	18:3, AZA	ND	ND			
PG	**18:3, 16:1**	5,760 ± 1,036	6,583 ± 794	1.1		
	HO-18:3, 16:1	33 ± 7	137 ± 19	4.2	0.6	2.1
	18:3, 16:0	5,405 ± 817	8,046 ± 1,472	1.5		
	HO-18:3, 16:0	42 ± 9	221 ± 30	5.3	0.8	2.7
TG	**18:3, 18:3, 18:3**	178 ± 19	1,715 ± 424	9.6		
	HO-18:3, 18:3, 18:3	0.49 ± 0.14	223 ± 98	455	0.03	13.0
	HO-18:3, HO-18:3, 18:3	ND	6.3 ± 2.1			0.4
TG	**18:3, 18:3, 18:2**	289 ± 37	1,976 ± 416	6.8		
	HO-18:3, 18:3, 18:2	1.4 ± 0.3	227 ± 98	162	0.5	11.5
	HO-18:3, HO-18:3, 18:2	ND	5 ± 1.9			0.25
TG	**18:3, 18:3, 16:0**	33 ± 4	367 ± 105	11.1		
	HO-18:3, 18:3, 16:0	0.7 ± 0.2	136 ± 55	194	2.1	37.0
	HO-18:3, HO-18:3, 16:0	ND	4 ± 1			1.1
TG	**18:3, 18:2, 16:0**	114 ± 16	1,153 ± 379	10.1		
	HO-18:3, 18:2, 16:0	1.4 ± 0.3	141 ± 46	101	1.2	12.2
PI	**18:3, 16:0**	1,193 ± 191	2,475 ± 484	2.1		
	HO-18:3, 16:0	15 ± 3	122 ± 18	8.1	1.3	4.9
PC	**18:3, 18:3**	2,145 ± 189	1,524 ± 252	0.7		
PC	**18:3, 18:2**	697 ± 117	455 ± 65	0.7		
PC	**18:3, 16:0**	470 ± 54	221 ± 24	0.5		
PE	**18:3, 16:0**	601 ± 66	1,223 ± 109	2.0		

Thereafter, levels of [2,2-D_2]AZA decreased while levels of [2,2-D_2]PIM further increased, reaching levels of 4 and 232 nmol g^{-1} dry weight, respectively, after 24 h (Fig. 4A). Labeled ONA, AZA, and PIM were not incorporated into galactolipids. These results indicate that, after uptake, ONA is instantaneously metabolized to AZA, which in turn is degraded by β-oxidation to PIM. When unlabeled AZA (100 μM) was fed to the seedlings, transient accumulation of AZA followed by β-oxidation to PIM was observed. AZA was not found to be incorporated into MGDG (Fig. 4B). We could not detect 9-hydroxynonanoic acid or ONA in any of the application experiments, indicating that reduction of the aldehyde or AZA is not a significant metabolic pathway in Arabidopsis. The results suggest that biogenesis of AZA and PIM starts in plastids, where ONA and OHA esterified in galactolipids are generated through free radical-catalyzed oxidative fragmentation of polyunsaturated C18 and C16 fatty acids. Further free radical-catalyzed oxidation of esterified ONA and OHA leads to an accumulation of esterified AZA and PIM in galactolipids. Hydrolytic release of fragmented fatty acids by lipases may then result in the accumulation of free AZA and PIM. During galactolipid hydrolysis, ONA and OHA may also be liberated. However, these oxo-acids do not accumulate in free form and are rapidly converted into AZA and PIM (Fig. 4), most likely through aldehyde dehydrogenases.

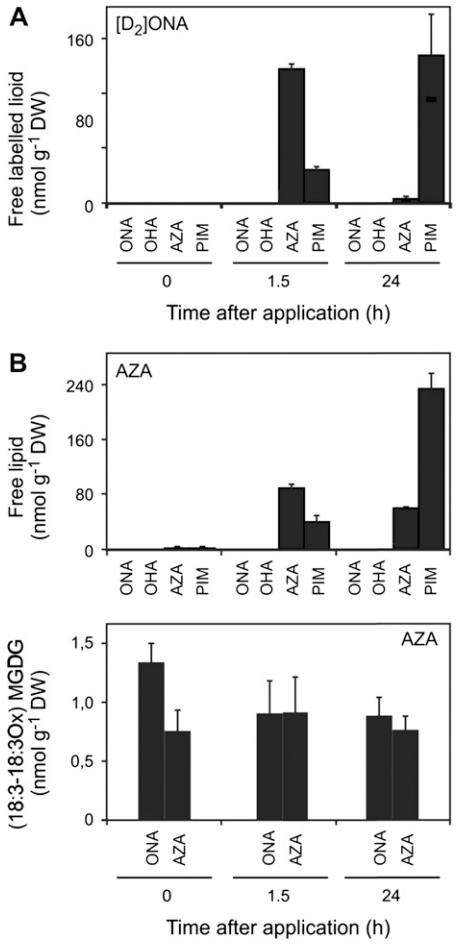

Figure 4. Metabolism of ONA and AZA. Arabidopsis seedlings were grown in liquid medium for 10 d. A, After exogenous application of [8,8-D_2]ONA, endogenous levels of free ONA, OHA, AZA, and PIM were determined. B, After exogenous application of AZA, levels of free ONA, OHA, AZA, and PIM as well as levels of oxidized (18:3,18:3)MGDG containing esterified ONA and AZA were measured. Values shown are means ± SD (n = 3). DW, Dry weight.

LPO Mechanisms: $^1O_2$-, Free Radical-, and LOX-Catalyzed Membrane Peroxidation Is Triggered by *Pst*

We next addressed the question of which mechanisms of LPO are involved in the formation of glycerolipid peroxides in vivo. Accumulation of glycerolipid peroxides is essential for and precedes free radical-catalyzed lipid fragmentation (Supplemental Fig. S3). The contribution of $^1O_2$-, free radical-, and LOX-mediated peroxidation to total LPO was assessed by fatty acid peroxide fingerprinting [i.e. by determining the free and esterified HO(O)-18:3 fatty acid isomer composition in Arabidopsis Col-0 leaves; Mueller et al., 2006; Triantaphylidès et al., 2008]. Leaves from 6-week-old plants were mock infiltrated (control) or infected with avirulent *Pst* (10^8 cfu mL^{-1}), harvested 24 h after treatment, immediately shock frozen, and extracted under peroxide-reducing conditions, thereby converting lipid peroxides into the corresponding stable hydroxides. Reducing conditions proved to be essential to prevent degradation and artifact formation, thereby yielding higher recovery of oxidized lipids as compared with previous studies (Ibrahim et al., 2011; Vu et al., 2012). HO-18:3 isomers were determined in lipid extracts in free form as well as in esterified form (after release from complex lipids by alkaline hydrolysis) by UPLC-MS/MS (Supplemental Fig. S6). Levels of free HO-18:3 were 1% or less of the levels of esterified HO-18:3 under control conditions and after infection (Fig. 5A), indicating that glycerolipids are the major targets for fatty acid peroxidation. From the HO-18:3 isomer pattern (Supplemental Figs. S4 and S5), levels of HO(O)-18:3 formed through $^1O_2$, free radical oxidation, and LOXs (Fig. 5A) could be calculated (Triantaphylidès et al., 2008). Under control conditions, the observed isomer pattern of esterified HO-18:3 is indicative for a prevalent $^1O_2$-dependent oxidation mechanism (more than 90 mol %). HO-18:3 derived from free radical-catalyzed oxidation and 13-LOX comprised 3 and 7 mol % of all esterified HO-18:3, respectively (Fig. 5A). After *Pst* infection, levels of esterified HO-18:3 oxidized by $^1O_2$, free radicals, and 13-LOX increased by 2.9-, 43-, and 56-fold, and the relative contribution of $^1O_2$, free radicals, and 13-LOX to overall HO-18:3 formation changed to 40%, 18%, and 40%, respectively.

LOX2 Is Central for LOX-Mediated Glycerolipid Peroxidation and Modulates the Levels of Free HO Fatty Acids after Pathogen Infection

LOX2 has been shown to be involved in the formation of arabidopsides from MGDG and DGDG in plastids (Glauser et al., 2009; Seltmann et al., 2010). Analysis of the total 13-HO(O)-18:3 pattern in the *lox2* mutant revealed that LOX2 is responsible for virtually all the LOX-mediated synthesis of esterified 13-HO(O)-18:3 under control (100%) and pathogen-induced (93%) conditions (Fig. 5B). This result suggests that LOX2 may directly oxidize galactolipids.

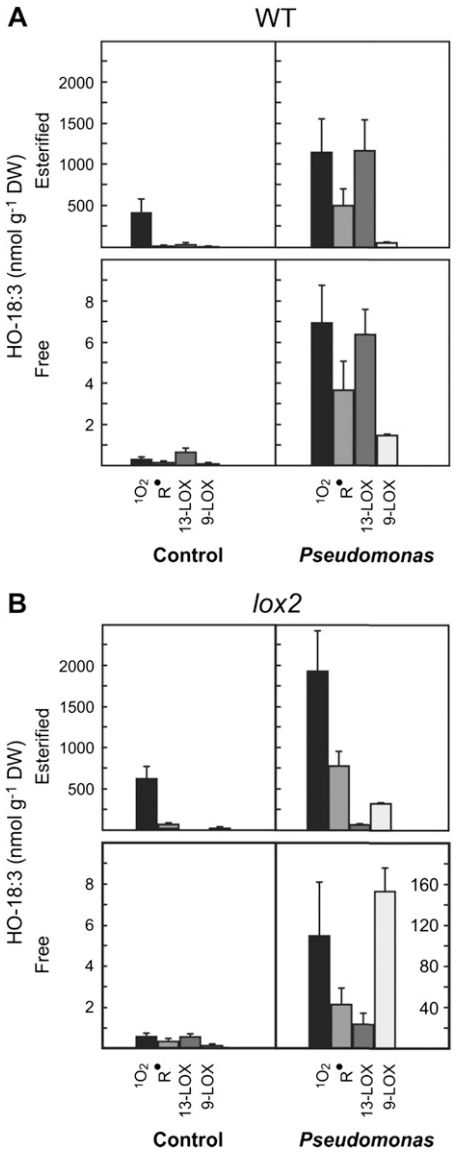

Figure 5. Mechanisms of 18:3 oxidation in Arabidopsis leaves after infection with avirulent *Pst*. Levels of esterified and free HO(O)-18:3 generated by $^1O_2$ oxidation, free radical catalysis, and 9-LOX or 13-LOX catalysis are shown for wild-type (WT; A), and *lox2* mutant (B) plants under control conditions (mock infiltration) and 24 h after infection with avirulent *Pst* (10^8 cfu mL^{-1}). Note the different scales of the vertical axes. Values shown are means ± SD (n = 3). DW, Dry weight.

To this end, pathogen-triggered oxidation of MGDG and DGDG was analyzed in wild-type and *lox2* mutant plants by UPLC-MS/MS after reduction of lipid peroxides to the corresponding hydroxides. In the wild type, levels of galactolipids in which both acyl chains were peroxidized (dihydroperoxides) dramatically increased in a LOX2-dependent manner, while galactolipids with one peroxidized acyl chain (monohydroperoxides) showed only a minor increase that was not dependent on LOX2 (Fig. 6B). However, dihydroperoxy galactolipids were not completely lacking in the *lox2* mutant (Fig. 6B). This finding is compatible with the hypothesis that galactolipid monohydroperoxides are formed through random $^1O_2$-mediated oxidation of acyl chains at the *sn1* or *sn2* position close to the production site of short-lived $^1O_2$, while dihydroperoxides are predominantly generated by direct double oxygenation of galactolipids by LOX2 (Fig. 6B). The later galactolipid dihydroperoxides may serve as direct precursors of arabidopsides that comprise two cyclooxylipin acyl chains (12-oxo-phytodienoic acid [OPDA] or dinor OPDA). In fact, a massive synthesis of arabidopsides was only observed in the wild type but not in the *lox2* mutant after *Pst* infection (Fig. 6C).

Arabidopsides A, B, G, and E accumulated to almost 50% of the initially present nonoxidized MGDG precursors, which should be accompanied by a dramatic loss of nonoxidized MGDG precursors. In contrast, a strong accumulation of the nonoxidized MGDG (2.4- to 3.3-fold increase) and DGDG (1.4- to 2.3-fold increase) was observed (Table I; Fig. 6A). This increase was detected both in the wild type and the *lox2* mutant. Hence, pathogen-triggered stimulation of lipid accumulation appears not to be a compensatory mechanism for LOX2-mediated lipid consumption.

Unexpectedly, however, LOX2 appears to contribute to but not to be strictly required for the accumulation of free 13-HO(O)-18:3, free OPDA, and JA after pathogen infection (Fig. 6D). Since arabidopsides are virtually absent in the *lox2* mutant, arabidopsides are not essential precursors for the production of jasmonate signals after infection. Although LOX2 increases dihydroperoxide galactolipid levels after infection (Fig. 6B), no accumulation of galactolipids with two fragmented acyl chains could be detected. In addition, LOX2 appears to contribute to but not to be strictly required for the formation of fragmented fatty acids (Fig. 3B).

Compared with the wild type, surprisingly, the *lox2* mutation caused an excessive pathogen-induced 13- and 9-LOX activation, resulting in 2- and 80-fold higher accumulations of free 13- and 9-HO(O)-18:3 (Figs. 5B and 6B). In addition, also a dramatic pathogen-induced overaccumulation of nonenzymatically oxidized HO(O)-18:3 was observed in the *lox2* mutant (Fig. 5B). Notably, levels of free HO(O)-18:3 oxidized by $^1O_2$ and free radicals were both about 10-fold higher in the *lox2* mutant compared with the wild

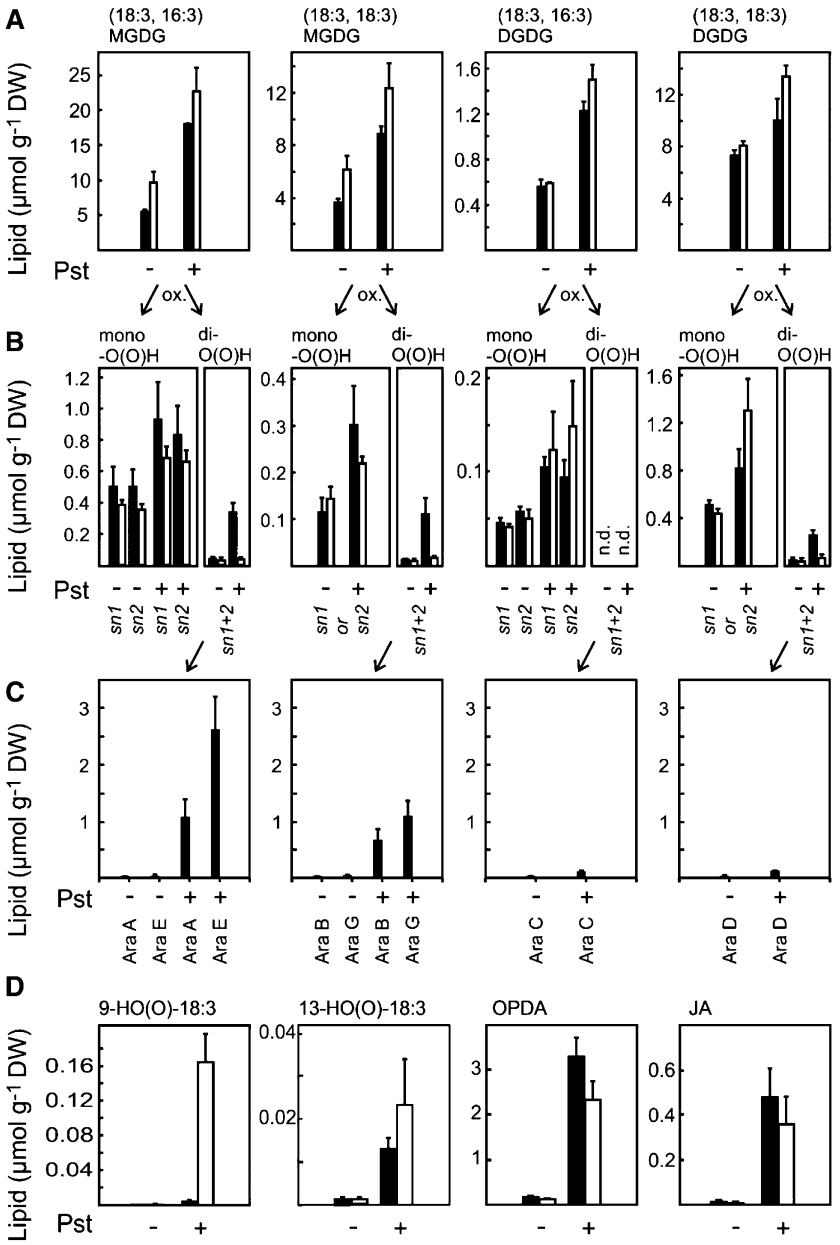

Figure 6. LOX2-dependent lipid accumulation and oxidation after infection with avirulent *Pst*. Arabidopsis leaves of wild-type (black bars) and *lox2* (white bars) plants were infected with avirulent *Pst* (10^8 cfu mL^{-1}; +) or mock infiltrated (−). Lipids were extracted 24 h after infection and analyzed by UPLC-MS/MS. Arrows indicate putative precursor-product relationships. Values shown are means ± SD of three independent experiments. A, Levels of the most abundant nonoxidized MGDG and DGDG species increased after infection in both genotypes. B, After infection, levels of monooxygenated (at the acyl chain in the *sn1* or *sn2* position) MGDG and DGDG species increased in a LOX2-independent manner, while the dioxygenated (at the acyl chains in the *sn1* and *sn2* positions) species accumulated in a LOX2-dependent fashion. C, Arabidopsides (Ara A–Ara G) were only detected in wild-type plants. Levels of arabidopsides strongly increased after infection. D, Levels of nonesterified 18:3 oxidation products. A strong overaccumulation of the 9-LOX product HO(O)-18:3 was observed in *lox2* mutant leaves, while levels of 13-LOX products [13-HO(O)-18:3, OPDA, and JA] increased in a LOX2-independent manner. DW, Dry weight.

type (Fig. 5) after infection. Hence, membrane oxidation by LOX2 reduces via an unknown regulatory mechanism the accumulation of nonenzymatically and enzymatically oxidized free fatty acids. Moreover, LOX2 and arabidopsides are not essential for the production of free jasmonates, at least in the late phase (24 h after infection) of the Arabidopsis-*Pst* interaction.

Galactolipids and TG Are Major Targets for Peroxidative Fatty Acid Modification

To identify the major targets of nonenzymatic LPO, lipid extracts were analyzed (after reduction of peroxides to the corresponding hydroxides) for the presence of complex lipids that comprised esterified HO-18:3 by UPLC-quadrupole-time of flight. Five classes of glycerolipids could be identified that comprised esterified HO-18:3: MGDG, DGDG, phosphatidylglycerols (PG), TG, and phosphatidylinositols (PI), while esterified HO-18:3 could not be detected in phosphatidylcholines (PC) and phosphatidylethanolamines (PE). All oxidized glycerolipids were found to be derived from the most highly abundant polyunsaturated glycerolipids within these lipid classes. A targeted analysis of nonoxidized glycerolipids and their corresponding HO-18:3 comprising species was performed by UPLC-MS/MS in the multiple reaction monitoring mode (for details, see "Materials and Methods").

Analysis of mock-infiltrated Arabidopsis leaves revealed that by far the most highly peroxidized glycerolipid species are (18:3, 16:3)MGDG, (18:3, 16:3) DGDG, and (18:3, 18:3)DGDG (Table I). Notably, total levels of oxidized versions of these species [comprising one or two HO(O) acyl chains] relative to the level of the corresponding nonoxidized galactolipid species were 19, 18, and 7 mol %, respectively. In contrast, basal levels of oxidized (18:3, 18:3)MGDG, PG, PI, and TG species were between 0.5 and 2.1 mol % (Table I).

After *Pst* infection, levels of all peroxidized lipid species of MGDG, DGDG, PG, and PI increased about 2- to 8-fold. Notably, a 100- to 455-fold increase of HO(O)-18:3 comprising TG species was observed. Under basal conditions, the degree of lipid oxidation of polyunsaturated TG species was between 0.03 and 2.1 mol % (relative to the nonoxidized precursor species). However, several TG species became highly oxidized after pathogen infection, and the degree of oxidation increased to 11 to 37 mol %.

Accumulation of oxidized lipids did not reduce the pool size of their nonoxidized precursor lipids. In contrast, *Pst* infection induced a massive accumulation of polyunsaturated MGDG, DGDG, PG, PE, PI, and TG species, while PC species became less abundant. The most dramatic accumulation of lipids was observed within the TG lipid pool, with a 7- to 10-fold mass increase (Table I). This increase was observed only in infected leaves but not in noninfected leaves of the same plant (Supplemental Fig. S7). It is not clear if this accumulation in infected leaves (displaying severe leaf damage after 24 h) results from disturbed lipid catabolism or increased synthesis. All lipids analyzed are from plant origin, since *Pst*, like most bacteria (except for cyanobacteria), cannot synthesize glycerolipids comprising trienoic fatty acids and galactolipids.

DISCUSSION

LPO in the Arabidopsis-*Pst* Interaction

Oxidative stress and LPO are well-known consequences of a variety of abiotic and biotic stresses. However, the predominant ROS species and LOXs involved in membrane LPO as well as the major site(s) of LPO in plant-pathogen interactions remained largely unknown for decades. On the one hand, enzymatic and nonenzymatic formation of low levels of ROS and LPO products in the early stages of the hypersensitive response (HR) have been implicated in processes such as defense signaling (Torres et al., 2006; Mueller et al., 2008), plant stress adaptation (Mueller, 2004), and SAR (Jung et al., 2009). The HR is characterized by an oxidative burst initiated by NADPH oxidases that produces superoxide anion radicals at the cell membrane (Torres et al., 2005). NADPH oxidases have been regarded as the major source of ROS species in plant-pathogen interactions involved in both signaling and LPO (Torres, 2010). However, NADPH oxidase-produced superoxide anion radicals (and their dismutation product hydrogen peroxide) are not sufficiently reactive to directly oxidize lipids (Frankel, 2005). Moreover, early NADPH oxidase activation within minutes at the cell membrane (Torres, 2010) does not coincide with LPO observed in plastid lipids (Table I) several hours after infection (Fig. 2). On the other hand, ROS-mediated excessive LPO is associated with membrane damage and, hence, may contribute to the execution of the cell death program (5–24 h after infection).

We show that $^1O_2$ is a major ROS involved in basal LPO and pathogen-induced LPO (Fig. 5). The remarkably high basal (8–19 mol %) and specific peroxidation of three major plastid galactolipids located close to the major site of $^1O_2$ production (i.e. PSII) might be due to the short half-life and high reactivity of $^1O_2$ (Triantaphylidès et al., 2008). After initiation of the HR process, photosynthetic activity is reduced (Berger et al., 2007) and progressive disorganization of the photosynthetic apparatus leads to increased $^1O_2$ formation and $^1O_2$-mediated LPO (Fig. 5).

For the most part, the increase of LPO is due to LOX2-mediated double oxygenation of plastid galactolipids (dihydroperoxides) that are rapidly converted into arabidopsides (Fig. 6). It has been proposed that arabidopsides serve as OPDA storage molecules, from which OPDA can be rapidly mobilized to generate jasmonate signals (Kourtchenko et al., 2007). However, LOX2 and arabidopsides were not found to be major sources of free jasmonates during the HR after *Pst* infection (Fig. 6), suggesting that one or more of LOX3, -4, and -6 are responsible for jasmonate accumulation under these conditions. In contrast, LOX2 appears to produce the majority of free jasmonates after wounding (Glauser et al., 2009) and during natural or dark-induced senescence (Seltmann et al., 2010). Despite the high LOX2-dependent jasmonate and arabidopside accumulation after wounding, LOX2 was not found to be required for JA signaling (Glauser et al., 2009) and appears to serve other functions.

Surprisingly, we found that nonenzymatic lipid oxidation as well as the enzymatic 9-LOX pathway (Fig. 5B) were dramatically increased in the *lox2* mutant, and higher LPO appeared to be associated with slightly increased visible leaf damage after infection with avirulent bacteria (Supplemental Fig. S1). Pretreatment of Arabidopsis leaves with 9-LOX products has been shown to protect the leaves against infection with virulent *Pst* DC3000 bacteria but not with avirulent *Pst* DC3000 *avrRpm1* bacteria (Vincente et al., 2011). Hence, activation of the 9-LOX pathway in *lox2* mutant plants may increase the local resistance against virulent bacteria, although this hypothesis remains to be tested. The mechanism of how LOX2-mediated membrane oxidation modulates total LPO levels also remains to be elucidated.

In addition to $^1O_2$ and LOX2, free radicals contribute significantly to LPO during *Pst* infection (Fig. 5). Radical-catalyzed LPO is low under basal conditions but becomes a major ROS-mediated LPO process during the HR (Fig. 5). Free radical-catalyzed LPO appears to take

place predominantly in plastid lipids, since we could detect marker lipids for free radical-catalyzed oxidation (fragmented fatty acids) in galactolipids but not in other glycerolipids (Table I). Hence, we determined that membrane LPO by all three LPO mechanisms (LOX2, $^1O_2$, and free radicals) is predominantly confined to plastid membranes. This result is in line with the light dependency of the HR in plant-pathogen interactions (Zeier et al., 2004; Montillet et al., 2005).

Biogenesis of AZA and PIM by Free Radical-Catalyzed Fragmentation of Fatty Acid Hydroperoxides in Arabidopsis

Lipid peroxides and hydrogen peroxide readily generate hydroxyl radicals in the presence of trace amounts of free transition metals (such as Cu^{2+} or Fe^{2+}) that are thought to be released from damaged metalloproteins (Spiteller, 2002). Another de novo source of hydroxyl radicals appears to be the lipid fragmentation process itself that is amplified during HR. The fragmentation mechanism of fatty acid hydroperoxides has recently been described by Schneider and coworkers in vitro and in animals in vivo (Schneider et al., 2008; Liu et al., 2011). In animals, fatty acid hydroperoxides and fragmented fatty acids accumulate in PC in the cellular membrane and in cardiolipins in mitochondrial membranes. Among the oxidized glycerolipids, oxidized PC containing ONA and AZA are the most abundant molecules (Podrez et al., 2002; Chen et al., 2008). The proposed fragmentation mechanism (Schneider et al., 2008; Liu et al., 2011) rationalizes the key findings of this study in Arabidopsis (Fig. 7): a precondition for the fragmentation process is the continuous formation and maintenance of a pool of galactolipid hydroperoxides through $^1O_2$-mediated LPO (Fig. 7A). For the second step to proceed, catalytic amounts of radicals are required to initiate peroxide dimer formation within the pool of peroxidized galactolipids. The third step is the spontaneous fragmentation of the dimer and the production of four products: core aldehydes (galactolipids containing an oxo-acid fragment such as ONA or OHA), short-chain aldehydes (such as hydroperoxynonadienal or hexenal), an oxidized (nonfragmented) glycerolipid radical, and hydroxyl radicals (the detailed fragmentation mechanism is shown in Supplemental Fig. S8). Hence, the fragmentation process itself dramatically amplifies de novo radical production. These radicals further oxidize oxo-acids in core aldehydes to core dicarboxylic acids (such as AZA and PIM) and catalyze the formation of a great variety of oxidized galactolipids. In fact, more than 50 species of oxidized galactolipids have been identified in Arabidopsis leaves thus far (Ibrahim et al., 2011; Vu et al., 2012). Oxidized and oxidatively fragmented galactolipids could represent a molecular memory of stress conditions and may serve as storage molecules for preformed oxylipins.

Our model also takes into account that oxidatively fragmented or polar acyl chains (such as ONA or AZA) protrude into the aqueous phase while nonoxygenated and monooxygenated fatty acids (such as in 13-HO-18:2) remain in the lipid phase, as determined by NMR studies (Li et al., 2007). It has been suggested that membranes thus "grow whiskers" according to the "lipid whisker model" (Greenberg et al., 2008). This conformational change of structural lipids during oxidation may contribute to the disruption of the membrane barrier and cell death (Fig. 7). In mammals, oxidized acyl residues protruding out of membranes will be selectively removed by specific

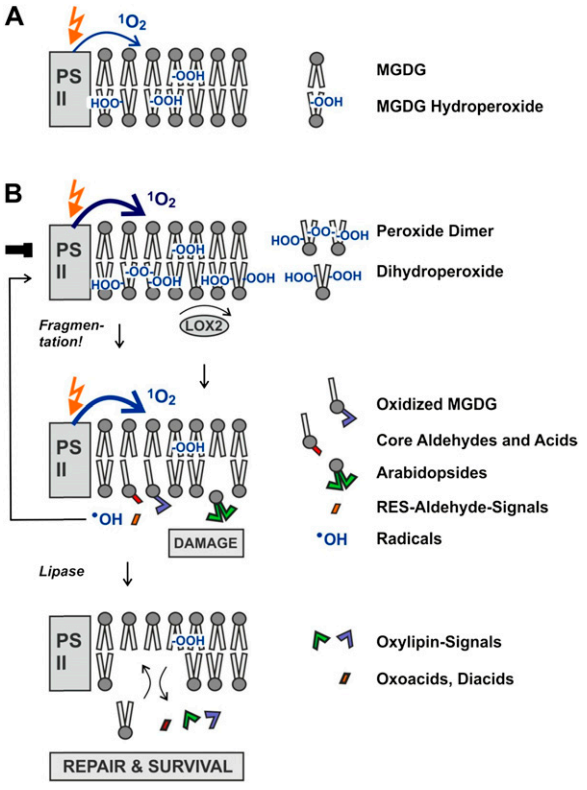

Figure 7. LPO and fragmentation in plastids (model). A, In the light, continuous $^1O_2$-mediated oxidation of MGDG close to PSII generates a pool of oxidation-sensitive MGDG hydroperoxides. B, Pathogen stress-induced inhibition of PSII in parallel with LOX2 activation increases MGDG peroxidation mediated by $^1O_2$ (MGDG monohydroperoxides) and LOX2 (MGDG dihydroperoxides). MGDG dihydroperoxides are rapidly converted into arabidopsides. MGDG monoperoxides are sensitive to radical-catalyzed formation of peroxide dimers that spontaneously break down, thereby generating oxidized MGDG and MGDG core aldehydes and acids that remain in the membrane as well as reactive electrophiles (RES) and radicals that are released instantaneously from the membrane. Mild membrane damage may stimulate repair and protection mechanisms through reactive lipid and oxygen species. However, excessive membrane damage caused by the amplification of LPO contributes to cell death. During membrane turnover and repair, oxidized MGDG, core aldehydes, and core acids are hydrolyzed, thereby releasing preformed biologically active oxylipins, oxo-acids, and diacids. Finally, oxidized lipids are replaced by de novo synthesis of lipids. [See online article for color version of this figure.]

repair lipases (Marques et al., 2002). In plants, specific repair lipases are not known; however, oxidized and fragmented fatty acids are ultimately released from galactolipids (Fig. 2).

Under basal conditions, total amounts of esterified ONA, OHA, AZA, and PIM are in the range of 229 nmol g^{-1} dry weight (Table I; Supplemental Fig. S4). Continuous formation, release, and rapid metabolism of these fragments to PIM (Fig. 4) may maintain a pool of free PIM (2–4 nmol g^{-1} dry weight; Fig. 2) that is essential for the biosynthesis of biotin (less than 1 nmol g^{-1} dry weight, as calculated by Shellhammer and Meinke [1990] in Arabidopsis leaves). Hence, fragmentation of galactolipids could be a general plant-specific and sufficient pathway to provide PIM to feed the biotin biosynthesis pathway.

Function of LPO and Fatty Acid Fragmentation

It has been proposed that nonenzymatic LPO protects plants from oxidative stress by scavenging ROS (Mène-Saffrané et al., 2009). Polyunsaturated galactolipids indeed scavenge large quantities of $^1O_2$ (Fig. 5; Table I) that escaped the carotenoid quenching mechanism (Ramel et al., 2012a), thereby preventing $^1O_2$-mediated protein damage. After pathogen infection, HO fatty acids derived from $^1O_2$-mediated LPO (Fig. 5; Grun et al., 2007) increase and have been shown to induce a strong accumulation of callose in Arabidopsis leaves, which is a frequent response of cells to pathogen assault (Vellosillo et al., 2010). Moreover, HO fatty acids derived from $^1O_2$-, radical-, or LOX-mediated LPO have been shown to up-regulate defense genes that are also up-regulated after *Pst* infection, suggesting a function of HO fatty acids in plant-pathogen defense responses (Vellosillo et al., 2007).

However, excessive or uncontrolled $^1O_2$-mediated LPO increases the vulnerability of lipids to overoxidation, lipid fragmentation, and de novo free radical production. It should be emphasized that hydroxyl radicals cannot be scavenged by polyunsaturated lipids. In contrast, a radical chain reaction propagates through membranes and ultimately leads to galactolipid and carotenoid fragmentation as well as radical amplification. Fragmentation of carotenoids leads to the formation of β-cyclocitral, which induces defense genes protecting against oxidative stress (Ramel et al., 2012b). Hence, LPO produces plastid lipid signals in the early stages of oxidative stress associated with high light and pathogen stress. However, massive LPO, exceeding a certain threshold level of oxidized lipids, may contribute to the execution of cell death (Triantaphylidès et al., 2008).

In animals, pathogen-induced lipid oxidation and fragmentation takes place in the cell membrane, enabling physical contact between pattern-recognition receptors of the Toll-like family and oxidized glycerolipids (Hazen, 2008). These receptors recognize in the first place pathogen surface lipids but also bind to endogenous oxidized surface lipids. Hence, in animals, oxidative stress activates the innate immune system by utilizing defense mechanisms evolved to fight pathogens (Binder et al., 2002). In plants, an immune function of oxidized glycerolipids has not been identified, while the biological activity of several free oxidized lipids has been well recognized.

In general, for free oxylipins, direct antimicrobial activity as well as signaling functions have been suggested (for review, see Matsui et al., 2006). Notably, oxidized and fragmented fatty acids are released from membranes in two waves (Fig. 7). During the first wave, fragmentation of oxidized lipids immediately generates reactive electrophile species oxylipins comprising short-chain aldehydes such as malondialdehyde and hexenal (Supplemental Fig. S8), which stimulate the expression of cell protection and rescue genes as well as many other genes commonly up-regulated in environmental stress and pathogenesis (Weber et al., 2004; Farmer and Davoine, 2007; Kishimoto et al., 2008). In addition, oxidation and fragmentation of galactolipids yield a pool of preformed esterified oxylipins. The activation of lipases, hence, results in the liberation of a second wave of (in part electrophilic) oxylipin signals and other oxidized lipids.

Among these free oxylipins with reported or proposed signaling functions are AZA (Jung et al., 2009; Shah, 2009; Chaturvedi et al., 2012), HO fatty acids (Vellosillo et al., 2007), and OPDA and phytoprostanes (Mueller at al., 2008). All of these oxidized lipids may contribute to the genetic reprogramming of metabolism and serve as damage-associated signals that induce detoxification and defense processes (Fig. 7). However, genetic evidence that these lipids play an essential role in the systemic immune response is scarce.

With respect to AZA, Jung et al. (2009) have proposed a function of free AZA as a phloem-mobile signal in priming the local and systemic immune responses in Arabidopsis. Although radiolabeled AZA infiltrated into leaves was shown to be transported through the phloem (Jung et al., 2009), we did not observe a systemic accumulation of AZA after infection with an avirulent *Pst* strain (Fig. 3; Supplemental Fig. S1). Moreover, we could not detect a specific induction of the *AZI1* gene by AZA treatment, and plant pretreatment with AZA also did not inhibit the growth of *Pst* DC3000 bacteria (Supplemental Fig. S2). Although we used similar experimental approaches to Jung et al. (2009), we could not confirm a general role of AZA in enhancing plant defense responses under our experimental conditions. In line with our results, Vincente et al. (2011) showed that AZA pretreatment displayed a barely detectable inhibition of the growth of *Pst* DC3000 bacteria in both pretreated and nontreated systemic leaves of the same plant. In addition, it was reported that lower bacterial densities resulted in better induction of SAR than high amounts and that the extent of tissue damage did not determine the extent of SAR (Mishina and Zeier, 2007). The fact that lower densities of bacteria led to lower levels of AZA also

argues against a role of AZA in SAR (Supplemental Fig. S1). Therefore, we rather suggest that AZA is a marker for free radical-induced lipid fragmentation associated with oxidative membrane damage and cell death (Fig. 2).

Several reactive electrophile species oxylipins such as OPDA and phytoprostanes induce the expression of genes related to detoxification and defense. A large proportion of gene regulation by OPDA and phytoprostanes is mediated by the TGACG motif binding (TGA) transcription factors TGA2, TGA5, and TGA6 (Mueller et al., 2008). A mutant defective in these three TGA factors is not able to display SAR (Zhang et al., 2003). However, this defect is more likely caused by the disturbance of SA signaling rather than by any disturbance of oxylipin signaling. The growth of this *tga2/5/6* mutant is more sensitive to toxic xenobiotics (Fode et al., 2008), suggesting that oxylipin signaling plays a role in detoxification metabolism. Clarification of the biogenesis of oxidized lipids as well as the identification of signaling factors specifically mediating the effects of oxidized lipids will enable a deeper understanding of the functions of these compounds in defense and signal transduction processes.

MATERIALS AND METHODS

Plant Material, Bacteria, and Growth Conditions

Arabidopsis (*Arabidopsis thaliana*) wild-type ecotypes Col-0 and Wassilewskija were grown in a growth chamber under a 9-h/15-h short-day cycle at 22°C/20°C (65% humidity, 120 μmol m^{-2} s^{-1}) in soil for 6 weeks. Mutant lines *lox2-1* and *lox1 lox5* were kindly provided by E. Farmer (Glauser et al., 2009); *fad3-2 fad7-2 fad8-1* was kindly provided by J. Browse (McConn and Browse, 1996); *azi1* (Salk_017709) was obtained from the Nottingham Arabidopsis Stock Centre (www.arabidopsis.org).

For pathogen infection, virulent and avirulent *Pseudomonas syringae* pv *tomato* DC3000 strains with/without avrRPM1 were used. Bacteria were cultured in King's B medium (40 g L^{-1} proteose peptone 3, 20 g L^{-1} glycerol, 10 mL L^{-1} $MgSO_4$ [10%, m/v], and 10 mL L^{-1} K_2HPO_4 [10%, m/v]) at 28°C with appropriate antibiotics. Bacterial suspension cultures were grown overnight, and cells were collected by centrifugation, washed, and resuspended in 10 mM $MgSO_4$.

For feeding experiments with fragmented fatty acids, Arabidopsis plants were grown in Murashige and Skoog liquid medium as described (Mueller et al., 2008). Experiments were performed with 10-d-old seedlings.

Chemicals and Plant Treatments

Chemicals and solvents were from Sigma, VWR, AppliChem, or Carl Roth if not stated otherwise and of the highest grade available. (18:0, 18:0)MGDG/DGDG were purchased from Matreya, TG from Larodan, and phospholipids from Avanti Polar Lipids.

Infiltration with bacteria or control treatment (10 mM $MgSO_4$) was conducted by syringe infiltration into the abaxial side of leaves. A bacterial suspension of optical density at 600 nm = 0.2 (10^8 cfu mL^{-1} suspension) was used.

Analysis of Oxidized Fatty Acids and Complex Lipids

Leaves from 6-week-old plants were harvested, immediately shock frozen, and extracted in the presence of the radical scavenger butylated hydroxytoluene (BHT) and the peroxide-reducing reagent triphenylphosphine (TPP). In a complex plant matrix, peroxidized lipids proved to be highly unstable compounds that are readily degraded during extraction and analysis. Therefore, the addition of both BHT and TPP proved to be essential to prevent degradation and artifact formation. For lipid profiling, fresh leaf material (300 mg; shock frozen in liquid nitrogen) was extracted with 2-propanol (1 mL) containing TPP (5 mg) and BHT (1.5 mg). The following internal standards were added: (18:0, 18:0)MGDG and (18:0, 18:0)DGDG (5 μg each), (10:0, 10:0, 10:0)TG (100 ng), (17:0, 17:0)PG (1 μg), (16:0, 16:0)PI (1 μg), (17:0, 17:0) phosphatidylserine (1 μg), (18:0, 18:0)PE (1 μg), (17:0, 17:0)PC (2 μg), dihydro-JA (100 ng), 15-HO-11,13(*Z*,*E*)-eicosadienoic acid (300 ng), and sebacic acid (100 ng). The sample was incubated for 15 min, sonicated for 5 min, and centrifuged. The supernatant was recovered, and the residue was further extracted with 1.5 mL of chloroform:2-propanol (1:2, v/v) followed by 1.5 mL of methanol:chloroform (1:2, v/v). The combined extracts were dried under a stream of nitrogen at 40°C and reconstituted in 100 μL of methanol containing 1 mM ammonium acetate for UPLC-MS/MS analysis.

UPLC-MS/MS analyses were performed on a Waters Micromass Quattro Premier triple quadrupole mass spectrometer with an electrospray interface coupled to an Acquity UPLC system (Waters). Galactolipid, jasmonate, and free and esterified HO fatty acid analyses were performed as described (Triantaphylidès et al., 2008; Seltmann et al., 2010). Phospholipid separation was carried out on a Waters UPLC BEH C18 column (2.1 × 50 mm, 1.7 μm with a 2.1 × 5 mm guard column) and eluted using a linear gradient (0.3 mL min^{-1} at 40°C) starting with 1 mM ammonium acetate in water:methanol (25:75, v/v) at 0 min to 0:100 (v/v) at 10 min. Free fragmented fatty acids were eluted using a linear gradient (0.3 mL min^{-1} at 40°C) starting with 0.1% acetic acid in water: methanol (95:5, v/v) at 0 min to 0:100 (v/v) at 10 min. For triacylglyceride analysis, a Waters UPLC BEH C8 column (2.1 × 50 mm, 1.7 μm with a 2.1 × 5 mm guard column) was eluted using a linear gradient (0.3 mL min^{-1} at 40°C) starting with 1 mM ammonium acetate in water:methanol (10:90, v/v) at 0 min to 0:100 (v/v) at 10 min. Lipids were analyzed in the positive (TG and PE) or negative (all other lipids) electrospray ionization mode (for details, see Supplemental Materials and Methods S1 and Supplemental Table S1).

Supplemental Data

The following materials are available in the online version of this article.

Supplemental Figure S1. Visible leave damage and increased levels of oxidized lipids in local but not in systemic leaves after infection with avirulent *Pst*.

Supplemental Figure S2. Lack of effect of AZA treatment on local defense responses against *Pst* DC3000 and expression of *AZI1*.

Supplemental Figure S3. Kinetics of $^1O_2$- and free radical-mediated fatty acid oxidation in vitro.

Supplemental Figure S4. Total levels of free and esterified fragmented fatty acids in Arabidopsis wild-type and *lox2* mutant plants.

Supplemental Figure S5. $^1O_2$- and free radical-mediated lipid oxidation in vitro.

Supplemental Figure S6. Isomer patterns of free and esterified HO(O)-18:3 in Arabidopsis wild-type and *lox2* leaves after infection with avirulent *Pst*.

Supplemental Figure S7. Increase of triglyceride levels in local but not in systemic leaves after infection with avirulent *Pst*.

Supplemental Figure S8. Nonenzymatic fragmentation mechanism of 9- and 13-HOO-18:3.

Supplemental Table S1. Mass transitions and conditions for electrospray ionization HPLC-MS/MS analysis.

Supplemental Materials and Methods S1.

ACKNOWLEDGMENTS

We thank K. Hess and D. Pezzetta for contributing AZI1 gene expression and systemic resistance tests.

Received July 2, 2012; accepted July 17, 2012; published July 22, 2012.

LITERATURE CITED

Berger S, Benediktyová Z, Matous K, Bonfig K, Mueller MJ, Nedbal L, Roitsch T (2007) Visualization of dynamics of plant-pathogen interaction by

novel combination of chlorophyll fluorescence imaging and statistical analysis: differential effects of virulent and avirulent strains of P. syringae and of oxylipins on A. thaliana. J Exp Bot **58:** 797–806

Binder CJ, Chang MK, Shaw PX, Miller YI, Hartvigsen K, Dewan A, Witztum JL (2002) Innate and acquired immunity in atherogenesis. Nat Med **8:** 1218–1226

Chaturvedi R, Krothapalli K, Makandar R, Nandi A, Sparks AA, Roth MR, Welti R, Shah J (2008) Plastid omega3-fatty acid desaturase-dependent accumulation of a systemic acquired resistance inducing activity in petiole exudates of Arabidopsis thaliana is independent of jasmonic acid. Plant J **54:** 106–117

Chaturvedi R, Venables B, Petros RA, Nalam V, Li M, Wang X, Takemoto LJ, Shah J (2012) An abietane diterpenoid is a potent activator of systemic acquired resistance. Plant J **71:** 161–172

Chehab EW, Kaspi R, Savchenko T, Rowe H, Negre-Zakharov F, Kliebenstein D, Dehesh K (2008) Distinct roles of jasmonates and aldehydes in plant-defense responses. PLoS ONE **3:** e1904

Chen X, Zhang W, Laird J, Hazen SL, Salomon RG (2008) Polyunsaturated phospholipids promote the oxidation and fragmentation of gamma-hydroxyalkenals: formation and reactions of oxidatively truncated ether phospholipids. J Lipid Res **49:** 832–846

Farmer EE, Davoine C (2007) Reactive electrophile species. Curr Opin Plant Biol **10:** 380–386

Fode B, Siemsen T, Thurow C, Weigel R, Gatz C (2008) The *Arabidopsis* GRAS protein SCL14 interacts with class II TGA transcription factors and is essential for the activation of stress-inducible promoters. Plant Cell **20:** 3122–3135

Frankel EN (2005) Lipid Oxidation, Ed 2. The Oily Press Lipid Library, Vol 18. PJ Barnes & Associates, Bridgwater, UK

Glauser G, Dubugnon L, Mousavi SA, Rudaz S, Wolfender JL, Farmer EE (2009) Velocity estimates for signal propagation leading to systemic jasmonic acid accumulation in wounded Arabidopsis. J Biol Chem **284:** 34506–34513

Greenberg ME, Li XM, Gugiu BG, Gu X, Qin J, Salomon RG, Hazen SL (2008) The lipid whisker model of the structure of oxidized cell membranes. J Biol Chem **283:** 2385–2396

Grun C, Berger S, Matthes D, Mueller MJ (2007) Early accumulation of non-enzymatically synthesized oxylipins in Arabidopsis after infection with Pseudomonas syringae. Funct Plant Biol **34:** 1–7

Hazen SL (2008) Oxidized phospholipids as endogenous pattern recognition ligands in innate immunity. J Biol Chem **283:** 15527–15531

Hazen SL, Chisolm GM (2002) Oxidized phosphatidylcholines: pattern recognition ligands for multiple pathways of the innate immune response. Proc Natl Acad Sci USA **99:** 12515–12517

Ibrahim A, Schütz A-L, Galano J-M, Herrfurth C, Feussner K, Durand T, Brodhun F, Feussner I (2011) The alphabet of galactolipids in Arabidopsis thaliana. Front Plant Sci **2:** 95

Jung HW, Tschaplinski TJ, Wang L, Glazebrook J, Greenberg JT (2009) Priming in systemic plant immunity. Science **324:** 89–91

Kirch HH, Schlingensiepen S, Kotchoni S, Sunkar R, Bartels D (2005) Detailed expression analysis of selected genes of the aldehyde dehydrogenase (ALDH) gene superfamily in Arabidopsis thaliana. Plant Mol Biol **57:** 315–332

Kishimoto K, Matsui K, Ozawa R, Takabayashi J (2008) Direct fungicidal activities of C6-aldehydes are important constituents for defense responses in Arabidopsis against Botrytis cinerea. Phytochemistry **69:** 2127–2132

Kourtchenko O, Andersson MX, Hamberg M, Brunnström A, Göbel C, McPhail KL, Gerwick WH, Feussner I, Ellerström M (2007) Oxophytodienoic acid-containing galactolipids in Arabidopsis: jasmonate signaling dependence. Plant Physiol **145:** 1658–1669

Li XM, Salomon RG, Qin J, Hazen SL (2007) Conformation of an endogenous ligand in a membrane bilayer for the macrophage scavenger receptor CD36. Biochemistry **46:** 5009–5017

Lin S, Hanson RE, Cronan JE (2010) Biotin synthesis begins by hijacking the fatty acid synthetic pathway. Nat Chem Biol **6:** 682–688

Liu W, Porter NA, Schneider C, Brash AR, Yin H (2011) Formation of 4-hydroxynonenal from cardiolipin oxidation: intramolecular peroxyl radical addition and decomposition. Free Radic Biol Med **50:** 166–178

López MA, Vicente J, Kulasekaran S, Vellosillo T, Martínez M, Irigoyen ML, Cascón T, Bannenberg G, Hamberg M, Castresana C (2011) Antagonistic role of 9-lipoxygenase-derived oxylipins and ethylene in the control of oxidative stress, lipid peroxidation and plant defence. Plant J **67:** 447–458

Marques M, Pei Y, Southall MD, Johnston JM, Arai H, Aoki J, Inoue T, Seltmann H, Zouboulis CC, Travers JB (2002) Identification of platelet-activating factor acetylhydrolase II in human skin. J Invest Dermatol **119:** 913–919

Matsui K (2006) Green leaf volatiles: hydroperoxide lyase pathway of oxylipin metabolism. Curr Opin Plant Biol **9:** 274–280

Matsui K, Minami A, Hornung E, Shibata H, Kishimoto K, Ahnert V, Kindl H, Kajiwara T, Feussner I (2006) Biosynthesis of fatty acid derived aldehydes is induced upon mechanical wounding and its products show fungicidal activities in cucumber. Phytochemistry **67:** 649–657

McConn M, Browse J (1996) The critical requirement for linolenic acid is pollen development, not photosynthesis, in an *Arabidopsis* mutant. Plant Cell **8:** 403–416

Mène-Saffrané L, Dubugnon L, Chételat A, Stolz S, Gouhier-Darimont C, Farmer EE (2009) Nonenzymatic oxidation of trienoic fatty acids contributes to reactive oxygen species management in Arabidopsis. J Biol Chem **284:** 1702–1708

Mishina TE, Zeier J (2007) Pathogen-associated molecular pattern recognition rather than development of tissue necrosis contributes to bacterial induction of systemic acquired resistance in Arabidopsis. Plant J **50:** 500–2513

Montillet JL, Chamnongpol S, Rustérucci C, Dat J, van de Cotte B, Agnel JP, Battesti C, Inzé D, Van Breusegem F, Triantaphylidès C (2005) Fatty acid hydroperoxides and H_2O_2 in the execution of hypersensitive cell death in tobacco leaves. Plant Physiol **138:** 1516–1526

Mosblech A, Feussner I, Heilmann I (2009) Oxylipins: structurally diverse metabolites from fatty acid oxidation. Plant Physiol Biochem **47:** 511–517

Mueller MJ (2004) Archetype signals in plants: the phytoprostanes. Curr Opin Plant Biol **7:** 441–448

Mueller MJ, Mène-Saffrané L, Grun C, Karg K, Farmer EE (2006) Oxylipin analysis methods. Plant J **45:** 472–489

Mueller S, Hilbert B, Dueckershoff K, Roitsch T, Krischke M, Mueller MJ, Berger S (2008) General detoxification and stress responses are mediated by oxidized lipids through TGA transcription factors in *Arabidopsis*. Plant Cell **20:** 768–785

Mukhtarova LS, Mukhitova FK, Gogolev YV, Grechkin AN (2011) Hydroperoxide lyase cascade in pea seedlings: non-volatile oxylipins and their age and stress dependent alterations. Phytochemistry **72:** 356–364

Podrez EA, Poliakov E, Shen Z, Zhang R, Deng Y, Sun M, Finton PJ, Shan L, Febbraio M, Hajjar DP, et al (2002) A novel family of atherogenic oxidized phospholipids promotes macrophage foam cell formation via the scavenger receptor CD36 and is enriched in atherosclerotic lesions. J Biol Chem **277:** 38517–38523

Ramel F, Birtic S, Cuiné S, Triantaphylidès C, Ravanat JL, Havaux M (2012a) Chemical quenching of singlet oxygen by carotenoids in plants. Plant Physiol **158:** 1267–1278

Ramel F, Birtic S, Ginies C, Soubigou-Taconnat L, Triantaphylidès C, Havaux M (2012b) Carotenoid oxidation products are stress signals that mediate gene responses to singlet oxygen in plants. Proc Natl Acad Sci USA **109:** 5535–5540

Schneider C, Porter NA, Brash AR (2008) Routes to 4-hydroxynonenal: fundamental issues in the mechanisms of lipid peroxidation. J Biol Chem **283:** 15539–15543

Seltmann MA, Stingl NE, Lautenschlaeger JK, Krischke M, Mueller MJ, Berger S (2010) Differential impact of lipoxygenase 2 and jasmonates on natural and stress-induced senescence in Arabidopsis. Plant Physiol **152:** 1940–1950

Shah J (2009) Plants under attack: systemic signals in defence. Curr Opin Plant Biol **12:** 459–464

Shellhammer J, Meinke D (1990) Arrested embryos from the bio1 auxotroph of *Arabidopsis thaliana* contain reduced levels of biotin. Plant Physiol **93:** 1162–1167

Spiteller G (2002) Do changes in the cell membrane structure induce the generation of lipid peroxidation products which serve as first signalling molecules in cell to cell communication? Prostaglandins Leukot Essent Fatty Acids **67:** 151–162

Torres MA (2010) ROS in biotic interactions. Physiol Plant **138:** 414–429

Torres MA, Jones JD, Dangl JL (2005) Pathogen-induced, NADPH oxidase-derived reactive oxygen intermediates suppress spread of cell death in Arabidopsis thaliana. Nat Genet **37:** 1130–1134

Torres MA, Jones JD, Dangl JL (2006) Reactive oxygen species signaling in response to pathogens. Plant Physiol **141:** 373–378

Triantaphylidès C, Krischke M, Hoeberichts FA, Ksas B, Gresser G, Havaux M, Van Breusegem F, Mueller MJ (2008) Singlet oxygen is the major reactive oxygen species involved in photooxidative damage to plants. Plant Physiol **148:** 960–968

Vellosillo T, Martínez M, López MA, Vicente J, Cascón T, Dolan L, Hamberg M, Castresana C (2007) Oxylipins produced by the 9-lipoxygenase pathway in *Arabidopsis* regulate lateral root development and defense responses through a specific signaling cascade. Plant Cell **19:** 831–846

Vellosillo T, Vicente J, Kulasekaran S, Hamberg M, Castresana C (2010) Emerging complexity in reactive oxygen species production and signaling during the response of plants to pathogens. Plant Physiol **154:** 444–448

Vincente J, Cascon T, Vicedo B, Garcia-Agustin P, Hamberg M, Castresana C (2011) Role of 9-lipoxygenase and alpha-dioxygenase oxylipin pathways as modulators of local and systemic defense. Mol Plant **5:** 914–928

Vu HS, Tamura P, Galeva NA, Chaturvedi R, Roth MR, Williams TD, Wang X, Shah J, Welti R (2012) Direct infusion mass spectrometry of oxylipin-containing Arabidopsis membrane lipids reveals varied patterns in different stress responses. Plant Physiol **158:** 324–339

Weber H, Chételat A, Reymond P, Farmer EE (2004) Selective and powerful stress gene expression in Arabidopsis in response to malondialdehyde. Plant J **37:** 877–888

Zeier J, Pink B, Mueller MJ, Berger S (2004) Light conditions influence specific defence responses in incompatible plant-pathogen interactions: uncoupling systemic resistance from salicylic acid and PR-1 accumulation. Planta **219:** 673–683

Zhang Y, Tessaro MJ, Lassner M, Li X (2003) Knockout analysis of *Arabidopsis* transcription factors TGA2, TGA5, and TGA6 reveals their redundant and essential roles in systemic acquired resistance. Plant Cell **15:** 2647–2653